RESEARCH ARTICLE

# Dose-Dependent Metabolic Alterations in Human Cells Exposed to Gamma Irradiation

Yong-Kook Kwon[1], In Jin Ha[1], Hyun-Whee Bae[1,3], Won Gyo Jang[1,3], Hyun Jin Yun[2], So Ra Kim[2], Eun Kyeong Lee[2], Chang-Mo Kang[2]*, Geum-Sook Hwang[1,3]*

**1.** Integrated Metabolomics Research Group, Western Seoul Center, Korea Basic Science Institute, Seoul, 120-140, Republic of Korea, **2.** Division of Radiation Effect, Korea Institute of Radiological & Medical Sciences, Seoul, 139-706, Korea, **3.** Graduate School of Analytical Science and Technology, Chungnam National University, Daejeon, 305-764, Republic of Korea

*kangcm@kirams.re.kr (CMK); gshwang@kbsi.re.kr (GSH)

## Abstract

Radiation exposure is a threat to public health because it causes many diseases, such as cancers and birth defects, due to genetic modification of cells. Compared with the past, a greater number of people are more frequently exposed to higher levels of radioactivity today, not least due to the increased use of diagnostic and therapeutic radiation-emitting devices. In this study, ultra-performance liquid chromatography-quadrupole time-of-flight mass spectrometry (UPLC-QTOF-MS)-based metabolic profiling was used to investigate radiation- induced metabolic changes in human fibroblasts. After exposure to 1 and 5 Gy of $\gamma$-radiation, the irradiated fibroblasts were harvested at 24, 48, and 72 h and subjected to global metabolite profiling analysis. Mass spectral peaks of cell extracts were analyzed by pattern recognition using principal component analysis (PCA) and partial least squares-discriminant analysis (PLS-DA). The results showed that the cells irradiated with 1 Gy returned to control levels at 72 h post radiation, whereas cells irradiated with 5 Gy were quite unlike the controls; therefore, cells irradiated with 1 Gy had recovered, whereas those irradiated with 5 Gy had not. Lipid and amino acid levels increased after the higher-level radiation, indicating degradation of membranes and proteins. These results suggest that MS-based metabolite profiling of $\gamma$-radiation-exposed human cells provides insight into the global metabolic alterations in these cells.

## Introduction

Recently, humans have become exposed to more radiation, both natural and artificial. Exposure to natural radiation has increased due to destructive changes in the environment, such as depletion of the atmospheric ozone layer. Moreover, exposure to artificial radiation has increased due to its use in cancer therapy, medical test equipment (such as X-ray-emitting computed tomography (CT) scanners), waste from the nuclear power industry, and nuclear accidents [1]. Excessive exposure to radiation causes serious health problems, because the effects include a series of molecular-, cellular-, and tissue-level processes [2].

The effects of exposure to radiation are complex, so have been analyzed in an overall manner. Analyses of the complex responses induced by radiation require high-throughput data processes and have depended on various ''-omics'' platforms, such as transcriptomics, proteomics, and metabolomics. Transcriptomics [3,4] and proteomics [5,6] were first used to assess the effects of ionizing radiation, followed by metabolomics [7]. Such efforts have discovered radiation-induced perturbations of RNA and protein molecules and have been successful in developing concepts such as a threshold dose [3,5,8]. However, any understanding of the response to radiation from such analyses is incomplete without a study of the metabolome. Analyses of the metabolome facilitate characterization of complex phenotypes, because changes in metabolites reflect systemic responses to environmental or genetic interventions, and the number of metabolites investigated is lower than the number of genes or proteins in organisms [9,10].

A metabolomics approach as a nontarget global profiling analysis is becoming increasingly popular as a source of biomedical data using mass spectrometry (MS) and nuclear magnetic resonance (NMR). Many studies have reported biomarkers in biofluids (urine and serum) for exposure to radiation [2,11,12,13]. Some metabolomics studies based on ultra-performance liquid chromatography (UPLC), and gas chromatography-mass spectrometry (GC-MS) have reported metabolites from energy, purine, and pyrimidine metabolism as urinary biomarkers of radiation exposure in rodents [14,15,16,17]. It has been reported that LDL/VLDL and amino acid levels were increased in the sera of γ-irradiated mice [2]. Amino acid levels in the urine of rats were increased following radiation exposure [13]. Patterson *et al.* [7] analyzed water-soluble metabolites induced by radiation, and reported that levels of antioxidants and metabolites related to DNA synthesis were decreased.

In the present study, we investigated global metabolic responses to γ-radiation in human fibroblasts. The cells were subjected to γ-radiation doses of 1 and 5 Gy, and then harvested at 24, 48, and 72 h post irradiation. The changes in metabolites were investigated by MS-based metabolite profiling analysis. Our data suggest that the metabolic responses over time differed between cells exposed to lower (1 Gy) and higher (5 Gy)-level irradiation.

## Materials and Methods

### Chemicals and reagents

HPLC-grade water, acetonitrile, and methanol were purchased from Honeywell Burdick & Jackson (Morristown, NJ, USA), and formic acid (99% purity) was from Sigma-Aldrich (St. Louis, MO, USA).

### Cell culture, radiation exposure, and sample collection

Human primary cultured dermal fibroblasts (NF46) were purchased from Young Sciences Inc. and maintained in DMEM, supplemented with 10% fetal bovine serum (FBS), 100 U/mL penicillin, and 100 µg/mL streptomycin at 37℃ in a humidified, 5% $CO_2$ incubator. Cells were grown in 100-mm culture dishes to subconfluency (~80–90%) and subcultured 1:4. The cultured cells were exposed to γ-rays from a $^{137}$Cs γ-ray source at a dose rate of 2.73 Gy/min. Cells were collected at 24, 48, and 72 h after exposure to 1 and 5 Gy. Cells were harvested by trypsin-EDTA and enumerated using a TC20 Automated cell counter (Bio-Rad, Hercules, CA, USA). Harvested cells were washed with PBS once and centrifuged (500× $g$, 5 min, 4℃). Cell pellets were resuspended in 500 µL of cold DW and disrupted using an ultrasonicator (VCX-750, Sonics & Materials, Newtown, USA). The ultrasonication process was performed for 30 s at 150 W, consisting of repeated cycles of 0.5-s ultrasonication followed by 0.5-s rest. Samples were placed in an ice water bath during cell disruption. Samples were stored at −80℃ until analysis.

### Cell proliferation assay, MTT assay, LDH cytotoxicity detection assay, and DCFDA assay

#### Cell proliferation assay

Cells were seeded on 12-well plates ($4 \times 10^4$ cells/well) and incubated with/without treatment with γ-radiation. The TC20 Automated Cell Counter (Bio-Rad) was used to determine the cell number.

#### MTT assay

Cell viability was quantified using a colorimetric MTT assay that measures mitochondrial activity in cells. Briefly, cells seeded at a density of $4 \times 10^4$/well in a 12-well plate (Corning, Corning, NY, USA) were allowed to adhere overnight. Before cell harvest, aliquots of MTT stock solution were added to each well, and the plate was incubated at 37℃ in a humidified 5% $CO_2$ incubator. After 2 h, the medium was removed and the precipitated formazan crystals were dissolved by adding 500 µL of DMSO to each well. The microplates were shaken at room temperature for 30 min and the optical density of each well was measured at 560 nm.

**LDH cytotoxicity detection assay**

LDH released into cultured media was measured using the LDH cytotoxicity detection kit (Takara Bio Inc., Otsu, Japan).

**DCFDA assay**

A flow cytometer was used to determine ROS levels. For total cells, ROS generation was measured using a fluorescence probe, DCFDA (Molecular Probes-Invitrogen, Carlsbad, CA, USA). For mitochondria-related ROS levels, mitotracker MitoSOX (Molecular Probes-Invitrogen) was used.

## Metabolite extraction

To extract metabolites from the cells, two sequential extractions, with water and 80% methanol, were conducted. The collected fibroblasts were placed in a 1.5-mL tube. Each sample was mixed with 0.5 mL of water, and vortexed for 10 s, followed by centrifugation (13,000 × g, 10 min, 4℃). The upper layer was decanted to a fresh tube. The cell pellet was resuspended in 1 mL of methanol/water (4:1) and vortexed for 1 min, followed by centrifugation (13,000 × g, 10 min, 4℃). The 80% MeOH extraction was repeated. The upper layer was transferred in 500-µL aliquots to new 1.5-mL tubes. All supernatants were collected and then dried using a rotary evaporator. The dried metabolite pellets were redissolved in 450 µL of 50% MeOH and filtered through a 0.2-µm hydrophilic PTFE syringe filter (Millex, Millipore, Ireland).

## UPLC and MS analysis conditions

For analysis of the complex chemical components of human cells, an Acquity UPLC systems, including a binary solvent manager, sample manager, column heater, and photodiode array detector, was coupled with hybrid quadrupole time-of-flight tandem mass spectrometry UPLC-ESI/Q-TOF (ESI/Triple TOF 5600, AB SCIEX, Concord, ON, Canada). Chromatographic separation of samples was performed on AQUTIC UPLC HSS T3 column (2.1 mm × 100 mm, 1.7 µm) at 40℃ using water containing 0.1% formic acid (A) and acetonitrile containing 0.1% formic acid (B). The gradient elution program was isocratic 0.1% B for 2 min, 0.1–50% B at 2–5 min, 50–99.9% B at 5–15 min, and isocratic 99.9% B for 2 min, and then the initial conditions for 2 min. The flow rate was maintained at 0.35 mL/min.

Data acquisition was performed using a Triple TOF 5600 system with Turbo V sources and a Turbo ion spray interface. TOF MS data were acquired in positive (negative) using an ion spray voltage of 4.5 kV (−4.5 kV), nebulizer gas (Gas 1) of 50 psi, heater gas (Gas 2) of 60 psi, curtain gas (CUR) of 30 psi, a turbo spray temperature of 500℃, and declustering potential (DP) of 90 V (−90 V). MS and MS/MS data were gathered in positive mode by the UPLC-ESI/Q-TOF, a hybrid triple quadrupole time-of-flight mass spectrometer equipped with Turbo V sources and a Turbo ion spray interface. For TOF MS/MS data, information-dependent acquisition (IDA) was used with the following acquisition conditions:

survey scans of 250 ms, product ion scans of 100 ms, high-resolution mode, DP of 90 V (−90 V), collision energy (CE) of 30 V (−30 V), and collision energy spread (CES) of 15 V. The TOF MS and IDA scan was operated over the mass range of *m/z* 100–1200. TOF MS and product ion calibration were performed daily in both high-sensitivity and high-resolution modes before analysis. A total of 5 µl of 80% methanol solution as a blank and pooled aliquots from each cell extract as a quality control (QC) were injected every 10 samples.

## Data processing for UPLC-QTOF MS

UPLC-ESI/Q-TOF raw data files were converted to mzML format using the AB SCIEX MS data converter software (AB SCIEX). They were preprocessed using the MZmine 2.10 software, an open-source framework for processing of mass spectrometry-based molecular profile data [18]. First, each MS spectrum was imported and filtered using the ''Savitzky- Golay'' algorithm. The ''Baseline cut off'' algorithm was used for baseline correction of the filtered data. Peak detection was performed in the following three steps: first, the individual ions above the given noise level are detected in each mass spectrum, and a mass list is generated; second, chromatograms were formed by connecting consecutive ions that could be detected continuously over the scans; and third, these chromatograms were deconvoluted into individual peaks using the ''local minimum search'' algorithm. An isotopic peaks grouper was used to identify isotope patterns, and then additional isotopic peaks were removed from the peak list, except for the highest isotope. To match relevant peaks in the peak lists, peak list alignment was conducted with the ''Join aligner'' algorithm. Following alignment, ''Gap filling'' was done to correct a number of occasions containing missing peaks as a product of deficient peak detection or a mistake in the alignment of different peak lists.

Median-fold-change normalization was used to remove systematic variation between samples from experiments [19]. To decrease instrumental bias, such as noise and variation, the following two processes were used to filter reliable peaks. Background peak ions in raw data were eliminated based on the ratios of peak intensities of the QC to a blank (QC/blank >3). In addition, peaks showing large variations in QC were eliminated (CV >30%).

## Identification of metabolites

Metabolites were tentatively identified by connecting to various metabolite databases, such as HMDB, MassBank, LipidMaps, and METLIN [20,21,22,23]. The neutral mass was the primary term for database searching, within a tolerance. Isotopic pattern similarity can then be used as a second filter to select optimal candidates, by comparing the ratios of the detected isotopes and matching isotopes from the predicted isotopic pattern of the database compound. The fragment pattern of metabolites in experiments was compared with the corresponding fragment pattern in the databases as a third filter. Thus, the *m/z* of the precursor ion, isotope pattern matching, and fragment pattern similarity were

used for the identification of the metabolites. Because MS fragmentation of each individual molecule results in a unique MS/MS fingerprint, similarities between MS fragmentations of identified MS peaks and of non-identified MS peaks were calculated to find similar metabolites to non-identified MS peaks. Similarities were determined by a modified cosine calculation that took into account the relative intensities of the fragment ions as well as the precursor *m/z* differences between the paired spectra. Cosine threshold values were set to 0.5 for similarity of non-identified and identified peaks, whereby a cosine value of 1.0 indicates identical MS/MS spectra [24].

## Data analysis

Chemometric methods were used to characterize and visualize differences and similarities among the different species. Principal component analysis (PCA) is an unsupervised method that analyzes samples in the absence of information about the samples. Prior to PCA, all variables obtained from UPLC-MS data sets were scaled to unit variance (UV). Partial least squares-discriminant analysis (PLS-DA) was used to maximize class discrimination. PCA, and PLS-DA were conducted using SIMCA-P+ (ver. 12.0; Umetrics, Umea, Sweden). *K*- means clustering was performed using the MeV software (ver. 4.9.0). The Kruskal-Wallis test (non-parametric ANOVA) and Tukey test using ranks as the *post-hoc* test of the Kruskal-Wallis test were applied using R (ver. 2. 12. 0).

## Results

Human primary cultured dermal fibroblasts (NF46) were exposed to γ-radiation and incubated for 24, 48, and 72 h. There were 10 culture dishes in each group, with the exception of one group that comprised five because five culture dishes collected 72 h after exposure to 1 Gy became contaminated during incubation. The numbers of cells in the dishes, and numbers of culture dishes, are summarized in Table S1.

### Cell proliferation assay, MTT assay, LDH cytotoxicity detection assay, and DCFDA assay

Cell proliferation assay, MTT assay, LDH cytotoxicity detection assay, and DCFDA assay for total ROS levels in cells were performed (Figure 1). The results indicated that a large portion of cells maintained their viability after 72 h and only a few cells were dead after radiation exposure, which may be associated with growth retardation. Radiation may produce ROS, but this does not guarantee cell death. The effect of ROS in cells may differ according to the amount and time of exposure.
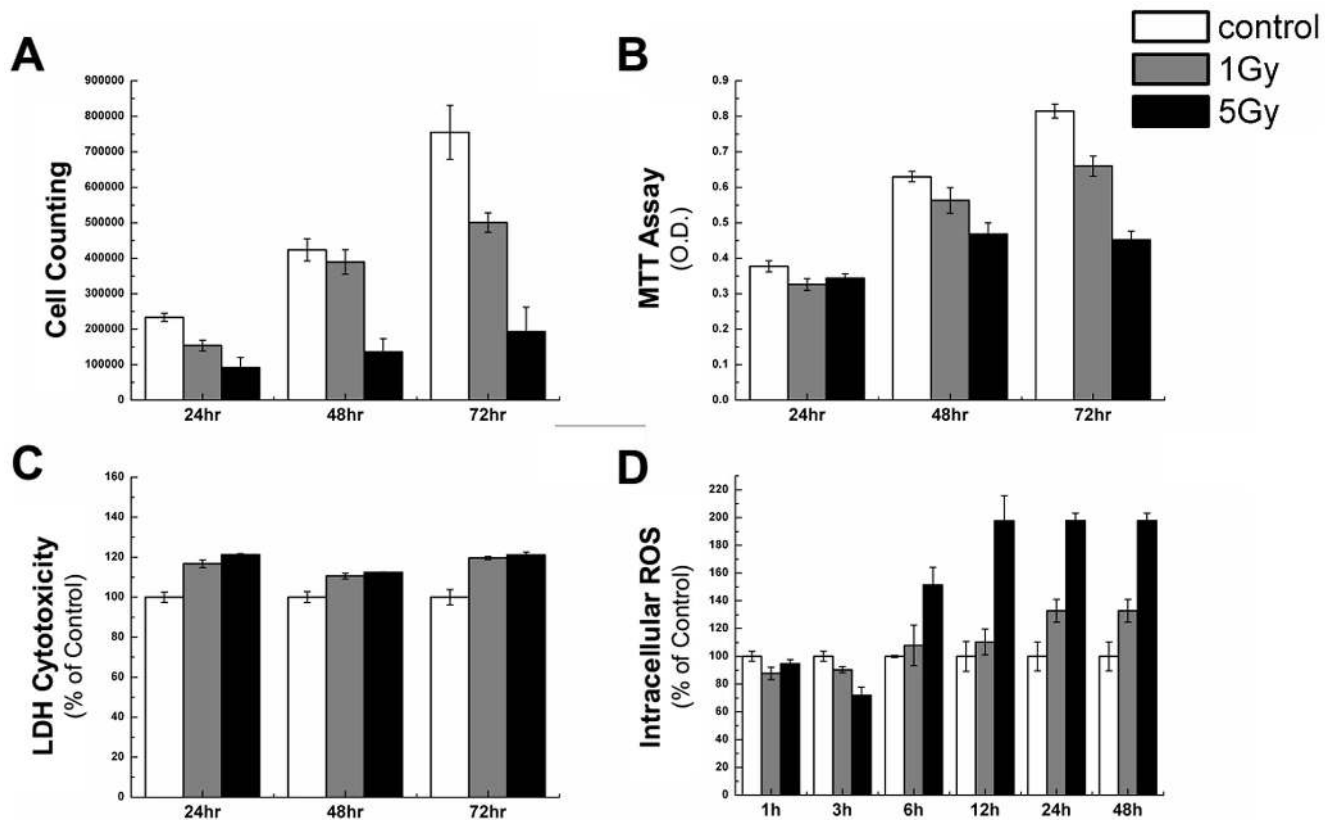
**Figure 1. A is from the cell proliferation assay, B from the MTT assay, C from the LDH cytotoxicity detection assay, and D from the DCFDA assay.**
Control, 1 Gy, and 5 Gy samples for cell numbers, MTT O.D., and LDH cytotoxicity were irradiated with mock, 1 Gy, and 5 Gy at 24, 48, and 72 h post radiation, in A, B, and C respectively; Control, 1 Gy, and 5 Gy samples for intracellular ROS were irradiated with mock, 1 Gy, and 5 Gy at 1, 3, 6, 12, 24, and 48 h post radiation, in D, respectively.

doi:10.1371/journal.pone.0113573.g001

## Multivariate analysis of MS data

The filtered peaks in positive and negative electrospray ionization (ESI) modes were used for further analyses. Prior to performing PCA for radiation effects, only control groups were analyzed to examine changes over 3days using PCA. The Results of PCA performed in control groups showed that the control groups were mixed with other groups (Figure S1). This suggested that metabolic changes in cells did not occur by 3 days. Three groups of control cells (24, 48, 72 h) were combined as the control since we wanted to examine the effect of radiation exposure on metabolites. Peaks having large variation in the control were eliminated to remove effects of time from the control (CV >40% in the control). PCA was then used to explore changes in samples after radiation. PCA showed that irradiated groups and controls could be distinguished post irradiation. The PCA score plots from mass spectral data of cell samples collected at 24, 48, and 72 h after irradiation are shown in Figure 2. PCA score scatter plots derived from mass spectral peaks in positive and negative ion mode did not show two separate groups. However, plots using PC 1 and 2 showed characteristic patterns, whereby
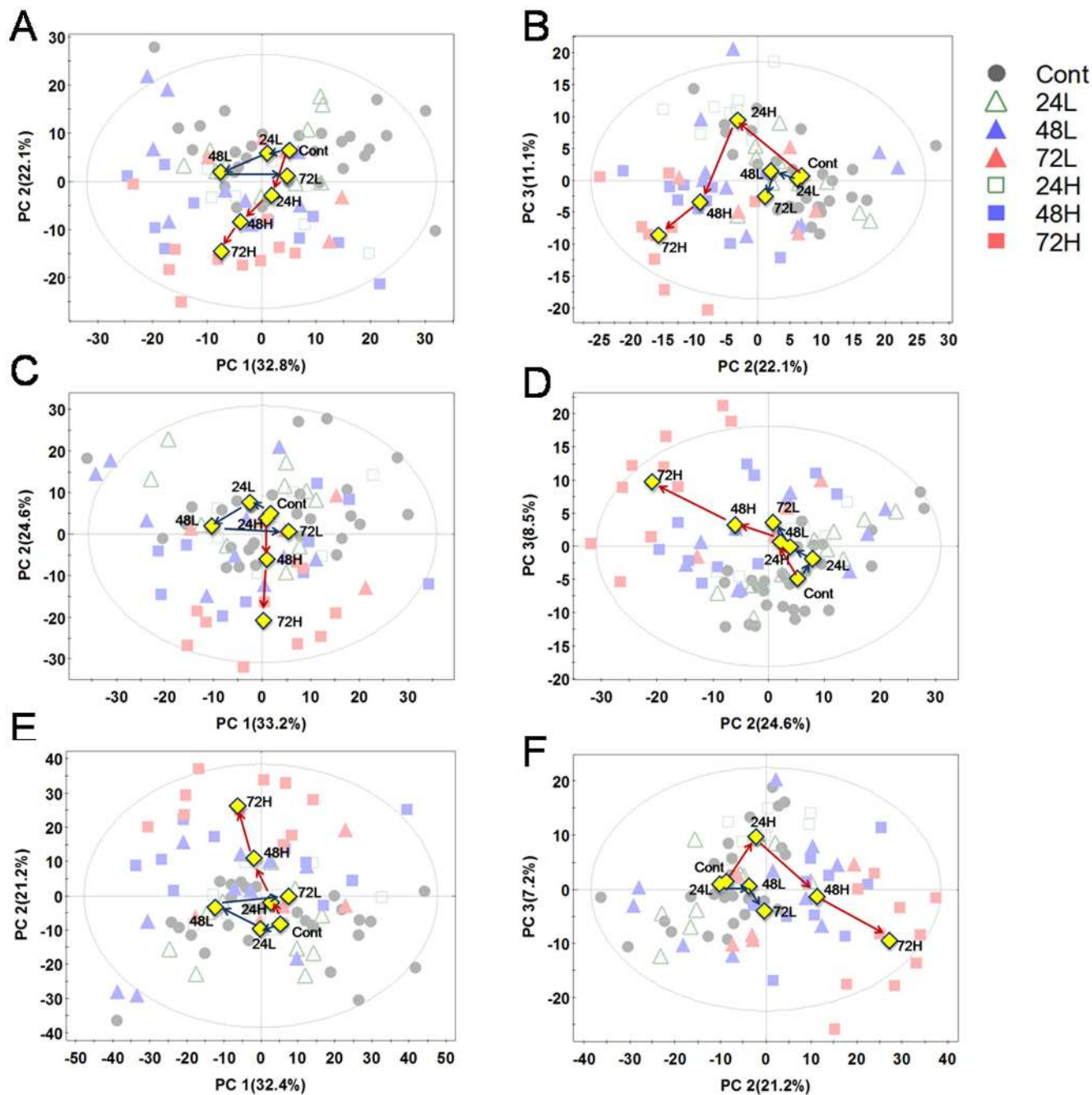
**Figure 2. PCA score plots were derived from UPLC-QTOF-MS.** A and B were from positive mode, C and D were from negative mode, and E and F were from the integration of positive and negative modes. Blue arrows and red arrows indicate the flow of cells irradiated with 1 and 5 Gy, respectively. Triangles and squares represent samples irradiated with 1 and 5 Gy, respectively. Yellow diamond marks indicate the averages of each group. Cont, control; 24L, 48L, and 72 L samples irradiated with 1 Gy at 24, 48, and 72 h post radiation, respectively.; 24H, 48H, and 72H samples irradiated with 5 Gy at 24, 48, and 72 h post radiation, respectively.

doi:10.1371/journal.pone.0113573.g002

the sample groups irradiated with the 5-Gy dose receded from the control group whereas sample groups irradiated with 1 Gy receded from and then returned to the control group ([Figure 2A, 2C](#)). In the PCA score plot using PC 2 and 3, both groups irradiated with 1 and 5 Gy receded from the control, but the samples irradiated with 5 Gy were further from the control than those that received 1 Gy ([Figure 2B, 2D](#)). Peaks from positive and negative ion modes were integrated to investigate the comprehensive changes in cells irradiated with 1 or 5 Gy. The PCA score plot from the integrated data was very similar to the plots in each ion mode ([Figure 2E, 2F](#)). The results of the PCA score plots of data in positive and negative ion modes and the integrated data showed that the pattern of metabolites detected in positive ion mode was similar to that in negative ion mode.

The PLS-DA technique was used to maximize the metabolite pattern among the groups. PLS-DA score plots showed clearer patterns, whereby the sample groups irradiated with 5 Gy receded from the control whereas the sample groups irradiated with 1 Gy receded and then returned to the control ([Figure 3](#)). The patterns in the PLS-DA plots were similar in models generated both using data in positive and negative ion modes and integrated data using both ion modes.

## Heatmap and k-means clustering

*K*-means clustering analysis was conducted to identify significant variables that affected changes in patterns in which the irradiated groups returned to control levels or receded from control groups over time (Figure S2; k=30). The levels of the variables included in clusters 7, 11, and 15 decreased after irradiation ([Figure 4A](#)). In the samples irradiated with 1 Gy, the level of variables in clusters 7, 11, and 15 recovered in the sample collected at 72 h post radiation. However, in the samples irradiated with 5 Gy, the levels of variables in the same cluster did not recover and decreased after radiation. Clusters 7, 11, and 15 involved 25, 72, and 129 variables, respectively.

The variables in cluster 19 and 24 were increased only in samples irradiated with 5-Gy γ- radiation ([Figure 4B](#)). The variables in cluster 19 were increased in samples irradiated with 5 Gy and collected at both 48 and 72 h post irradiation. However, those in cluster 24 were increased in samples irradiated with 5 Gy and collected at 72 h post irradiation. The variables in cluster 19 and 24 were increased slightly or unchanged in the cells irradiated with 1 Gy. In total, 74 and 100 variables were involved in clusters 19 and 24, respectively.

## Identification of metabolites

Lipids (PC(14:0/0:0), PC(16:0/0:0), PC(18:1/0:0), PE(p-16:0/0:0), PE(18:1/0:0), PE(16:1/0:0), PE(20:4/0:0), PE(22:6/0:0), and arachidonic acid), amino acids (glutamic acid, tryptophan, arginine, and tyrosine), amino acid derivatives (pyroglutamic acid, cysteinylglycine, glutathione, S-acetyl-L-methionine, and alloisoleucine), choline compounds (choline, cytidine 5′-diphosphocholine, glycerophosphocholine and O-phosphocholine), nucleotide compounds (uridine

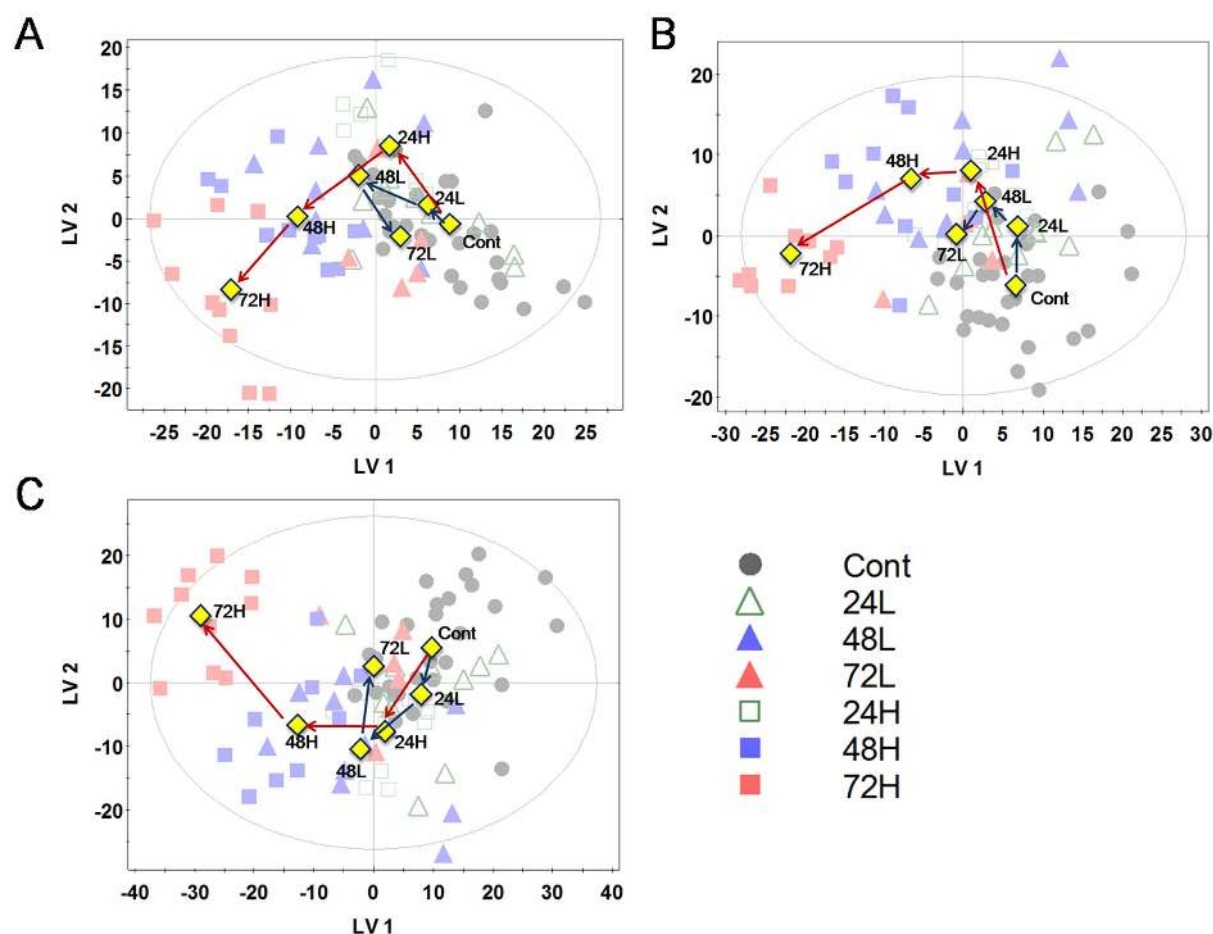**Figure 3. PLS-DA score plots from UPLC-QTOF-MS.** A is from positive mode, B is from negative mode, C is from the integration of positive and negative modes. (A. $R^2X$: 0.417, $R^2Y$: 0.182, $Q^2$: 0.105; B. $R^2X$: 0.429, $R^2Y$: 0.203, $Q^2$: 0.139; C. $R^2X$: 0.554, $R^2Y$: 0.276, $Q^2$: 0.204) Blue and red arrows indicate the flow of cells irradiated with 1 and 5 Gy, respectively. Triangles and squares indicate samples irradiated with 1 and 5 Gy, respectively. Yellow diamond marks indicate the averages of each group. Other symbols follow those in Figure 1.

diphosphate (UDP), UDP-Glc, UDP-GlcA and UDP-GalNAc, flavin adenine dinucleotide (FAD), and nicotinamide adenine dinucleotide (NAD)), and other metabolites (D-panthothenic acid, acetylneuraminic acid, justicidin B, hydroxybenzoic acid, citric acid, creatinine, and carnitinine) were identified in cell extracts using UPLC-QTOF-MS (Table 1). Relative quantification of metabolites was analyzed by using Kruskal-Wallis test to measure differences between each group. Prior to the Kruskal-Wallis test, groups were separated based on radiation dose. Identified metabolites were classified following the results of *k*-means clustering analysis (Figure S2). The quantitative information on metabolites is summarized in Table 2. We estimated putative classes of non-identified peaks through similarity of MSMS fragment patterns with identified peaks. The results are summarized in Table S2 and Table S3.

The metabolites in clusters 7, 11, 15, 19, and 24 in the results of the *k*-means clustering analysis were important to reveal the cellular response post irradiation.
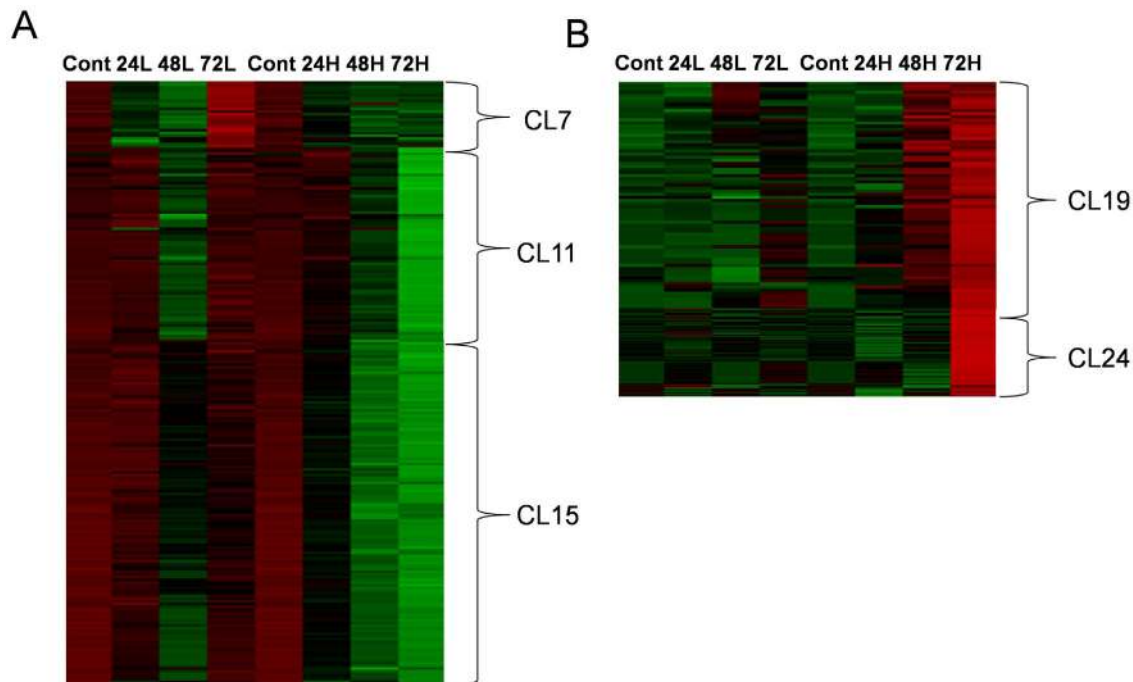
**Figure 4. Heat map of interesting clusters from *k*-means clustering analysis.** A: The clusters show the peaks that recovered from the decrease caused by radiation of 1 Gy. B: The clusters show peaks that increased 48 or 72 h after radiation with 5 Gy.

doi:10.1371/journal.pone.0113573.g004

Variables in clusters 7, 11, and 15 had recovered 72 h after radiation with 1 Gy, and variables in clusters 19 and 24 increased from 48 or 72 h after radiation with 5 Gy. Glutathione, cysteinylglycine, pantothenic acid (vitamin B5), and adenosyl-methionine were included in clusters 7 and 11. Several peaks having similar MS/MS patterns to vitamin B5 were included in cluster 11. PC class, PE class, tryptophan, choline, cytidine 5′-diphosphocholine, glycerophosphocholine, citrate, creatinine, and carnitine were included in cluster 19. Arachidonic acid, arginine, alloisoleucine, phenylalanine, tyrosine, and UDP-GalNAc were included in cluster 24. Some peaks that had similar MS/MS patterns to lipids (PC class, PE class, arachidonic acid), and amino acids (tyrosine, phenylalanine, and tryptophan) were included in cluster 19. Some peaks that had similar MS/MS patterns to amino acids (tyrosine, or arginine) were included in cluster 24. Representative metabolites of specific classes such as amino acids, lipids, and glutathione derivatives are shown in Figure 5.

## Discussion

According to our results, PCA and PLS-DA showed that the cells irradiated with 5 Gy γ-radiation moved away from the controls as time passed, but those irradiated with 1 Gy γ-radiation returned to the controls as time passed. That is, upon exposure to low-level radiation (1 Gy), the cells returned to a normal state or a

**Table 1.** List of metabolites identified from fibroblasts.

| Cluster | m/z | R.T. | Name | Formula | Adduction | Fragments |
|---------|-----|------|------|---------|-----------|-----------|
| 4 | 146.0462 | 0.8 | Glutamic acid | C5H9NO4 | [M−H]− | 102.06, 128.03,85.04 |
| 4 | 478.2911 | 10.59 | PE(18:1/0:0) | C23H46NO7P | [M−H]− | 281.25, 196.04,140.01 |
| 4 | 130.0489 | 0.8 | Pyroglutamic acid | C5H7NO3 | [M+H]+ | 84.04, 56.05,77.05 |
| 7 | 179.0476 | 1.19 | Cysteinylglycine | C5H10N2O3S | [M+H]+ | 76.02, 162.02,86.99 |
| 7 | 218.1032 | 4.73 | D-(+)-Pantothenic acid | C9H17NO5 | [M−H]− | 146.08, 88.04,71.05 |
| 7 | 308.0904 | 1.19 | Glutathione | C10H17N3O6S1 | [M+H]+ | 179.05, 162.02,76.02 |
| 9 | 308.0974 | 0.84 | N-Acetylneuraminic acid | C11H19NO9 | [M−H]− | 87.01, 170.04,98.06 |
| 9 | 565.0447 | 0.85 | UDP-Glc | C15H24N2O17P2 | [M−H]− | 323.03, 384.98,241.01 |
| 11 | 399.1434 | 0.84 | S-Adenosyl-L-methionine | C15H22N6O5S | [M+H]+ | 250.09, 136.06,298.1 |
| 12 | 784.1465 | 4.73 | FAD | C27H33N9O15P2 | [M−H]− | 437.09, 346.05,437.1 |
| 12 | 405.0086 | 0.96 | UDP | C9H14N2O12P2 | [M+H]+ | 97.03, 113.04,307.03 |
| 13 | 365.1046 | 0.89 | Justicidin B | C21H16O6 | [M+H]+ | 203.05, 185.04 |
| 13 | 450.2597 | 9.01 | PE(16:10/0:0) | C21H42NO7P | [M−H]− | 253.22, 196.04 |
| 16 | 137.0247 | 6.62 | p-Hydroxybenzoic acid | C7H6O3 | [M−H]− | 93.04, 66 |
| 19 | 162.1118 | 0.81 | Carnitine | C7H15NO3 | [M+H]+ | 103.04, 85.03,60.08 |
| 19 | 104.1064 | 0.75 | Choline | C5H14NO | [M]+ | 58.07, 60.08,59.08 |
| 19 | 191.0194 | 1.07 | Citric acid, anhydrous | C6H8O7 | [M−H]− | 111.01, 87.01,85.03 |
| 19 | 132.0761 | 0.89 | Creatine, anhydrous | C4H9N3O2 | [M+H]+ | 90.06, 90.9,87.08 |
| 19 | 489.1133 | 0.89 | Cytidine 5′-diphosphocholine | C14H26N4O11P2 | [M+H]+ | 264.04, 184.07,360.06 |
| 19 | 258.1095 | 0.79 | Glycerophosphocholine | C8H20NO6P | [M+H]+ | 104.11, 125,86.1 |
| 19 | 468.3074 | 7.84 | PC(14:0/0:0) | C22H46NO7P | [M+H]+ | 184.07, 104.11,450.3 |
| 19 | 496.3386 | 9.34 | PC(16:0/0:0) | C24H50NO7P | [M+H]+ | 184.07, 104.11,478.33 |
| 19 | 522.3542 | 9.73 | PC(18:1/0:0) | C26H52NO7P | [M+H]+ | 184.07, 125,504.34 |
| 19 | 500.2755 | 9.43 | PE(20:4/0:0) | C25H44NO7P | [M−H]− | 303.23, 196.04,259.24 |
| 19 | 524.2755 | 9.39 | PE(22:6/0:0) | C27H44NO7P | [M−H]− | 327.23, 283.24,196.04 |
| 19 | 436.2808 | 10.63 | PE(P-16:0/0:0) | C21H44NO6P | [M−H]− | 196.04, 239.24,140.01 |
| 19 | 203.083 | 4.79 | Tryptophan | C11H12N2O2 | [M−H]− | 116.05, 142.07,159.09 |
| 21 | 662.0985 | 1.04 | NAD | C21H27N7O14P2 | [M−H]− | 540.05, 408.01,272.96 |
| 21 | 184.0724 | 0.77 | O-Phosphocholine | C5H15NO4P | [M]+ | 125, 98.99,86.1 |

**Table 1.** Cont.

| Cluster | m/z | R.T. | Name | Formula | Adduction | Fragments |
|---------|------|------|------|---------|-----------|-----------|
| 21 | 579.0238 | 0.87 | UDP-GlcA | C15H22N2O18P2 | [M−H]− | 402.99, 323.03,254.99 |
| 24 | 303.2317 | 13.15 | Arachidonic acid | C20H32O2 | [M−H]− | 259.24, 205.2 |
| 24 | 175.1179 | 0.74 | Arginine | C6H14N4O2 | [M+H]+ | 70.07, 60.06,116.07 |
| 24 | 130.0878 | 2.28 | Alloisoleucine | C6H13NO2 | [M−H]− | 61.99, 97.93 |
| 24 | 164.0721 | 4.73 | Phenylalanine | C9H11NO2 | [M−H]− | 147.05, 103.06,91.06 |
| 24 | 182.0802 | 2.41 | Tyrosine | C9H11N1O3 | [M+H]+ | 136.08, 91.05,123.04 |
| 24 | 606.0713 | 0.86 | UDP-GalNAc | C17H27N3O17P2 | [M−H]− | 384.98, 282.04,402.99 |

doi:10.1371/journal.pone.0113573.t001

near-normal state rapidly. Upon exposure to higher-level radiation (5 Gy), the cells had not returned to a control state by 72 h after radiation exposure. Thus the cellular mechanisms that protect against stress were overwhelmed by exposure to higher-level γ-radiation. Although lymphoid cells such as TK6 readily undergo apoptosis after 24 h with radiation doses as low as 1.0 Gy [25], human fibroblasts exhibited a resistance to radiation in our experiment. Thus, the response to radiation differed according to cell type and species. Moreover, 1.0, 3.5, 6.5, or 8.5 Gy of total-body irradiation in nonhuman primates is equivalent to 0.76, 2.7, 5.0, and 6.5 Gy, respectively, in humans [26]. We have shown that 1 Gy induces transient metabolic changes in human fibroblasts. Since the levels of glutathione and glutathione derivatives recovered by 72 h after radiation exposure, glutathione may protect cells from damage by reducing oxygen free radical-induced oxidation. Although whether irradiation induces the same response in animal models remains unclear, analyses of the urines of irradiated mice have suggested that 0–8 Gy of gamma rays in mice [15,16,17], rats [14], and nonhuman primates [26] can induce systematic metabolic changes.

Glutathione, cysteinylglycine, pantothenic acid (vitamin B5), S-adenosyl-methionine, and two metabolites related to vitamin B5 decreased and then recovered in cells by 72 h after radiation with 1 Gy, but did not recover in cells irradiated with 5 Gy (Figure 5). Exposure of a cell to radiation can result in direct damage to DNA or indirect damage to genetic material through the radiolysis of water [27,28]. Glutathione is an antioxidant that prevents damage to important cellular components caused by reactive oxygen species, such as free radicals and peroxides [29]. Cysteinylglycine is derived from the breakdown of glutathione [30,31]. S-adenosyl-methionine is produced from adenosine triphosphate and methionine by methionine adenosyltransferase, and is an intermediate from methionine to glutathione [32]. Levels of cysteinylglycine and S-adenosyl-methionine are highly related to the level of glutathione. Changes in the levels of glutathione, cysteinylglycine, and S-adenosyl-methionine suggest that the

**Table 2.** Relative quantification of metabolites identified in human fibroblasts.

| Name | Cont | 24L | 48L | 72L | 24H | 48H | 72H | Post hoc (1 Gy) | Post hoc (5 Gy) |
|---|---|---|---|---|---|---|---|---|---|
| Glutamic acid[#,*] | 4977.4±1576.9 | 5604.2±1654.2 | 6874.1±1384 | 7512.4±1211.8 | 7390.7±1691.3 | 8236.2±1370.3 | 6720.5±1735.2 | c,d,f | c,e,f |
| PE(18:1/0:0)* | 1748.3±448.1 | 1846.2±554.2 | 1751.2±408.1 | 1736.1±441.7 | 2270.3±578.7 | 2329.4±691.4 | 2149.1±486 | | c,e |
| Pyroglutamic acid* | 131.9±31.2 | 156.8±32.9 | 160.2±38.3 | 171±33.5 | 177.4±32.7 | 206.5±23.5 | 180.5±46.5 | | c,e,f |
| cysteinylglycine[#,*] | 152.4±33.5 | 130.9±31.5 | 118.3±25.9 | 168.7±21.9 | 133.1±15.3 | 126.2±25.8 | 126.9±38.1 | d,e | e |
| D-(+)-Pantothenic acid[#] | 6817.9±1562.6 | 5419.5±1218 | 6323.5±1270.6 | 7031.1±803.4 | 6398.4±1239.2 | 6241.4±796.5 | 6020.6±1323.1 | c | |
| Glutathione[#] | 38771.4±11362.7 | 31348.3±7502.2 | 32677.6±8310.1 | 40767.2±7453 | 32805±4263.2 | 34234.7±9631.4 | 33988.2±13545.1 | e | |
| N-Acetylneuraminic acid* | 1493.9±205 | 1410.3±171.1 | 1360.2±176 | 1381.8±199.8 | 1332.5±181.5 | 1381±347.6 | 1267.6±195 | | f |
| UDP-Glc[#,*] | 13838.5±1768.8 | 12448.8±480.4 | 12695±1986.6 | 10664.8±1846.7 | 11958±2382.2 | 11989.5±1375.2 | 9663±1690.2 | f | e,f |
| S-Adenosyl-L-methionine[#,*] | 56.1±10.2 | 53.8±9.3 | 43.5±5.6 | 55.3±7.7 | 58.3±8 | 51.9±6 | 43.8±6.7 | a,d,e | b,f |
| FAD[#,*] | 431.2±63 | 401.9±62 | 383.2±54.5 | 347.1±39.3 | 372.1±38.8 | 349.2±69.7 | 422±33.5 | e,f | c,d,e |
| UDP* | 170±31.1 | 149.5±22.9 | 147.8±36.8 | 143.3±23.2 | 126±19.1 | 152.2±20.7 | 155.7±30.3 | | b,c |
| Justicidin B[#,*] | 53.5±18.5 | 81±25.1 | 47.1±17.9 | 26.4±12.6 | 66.7±8.1 | 50.9±34.9 | 34.9±8.1 | a,b,c,f | a,b,f |
| PE(16:1/0:0) | 231.1±58.8 | 240.2±66.9 | 185.2±54.1 | 196.4±61.9 | 246.3±55.4 | 289.2±99.6 | 230.9±48.8 | | |
| p-Hydroxybenzoic acid | 481.3±47.7 | 489.6±60.8 | 484.6±83.7 | 467.1±31.9 | 500.2±39.9 | 442.3±71.3 | 452.8±65.8 | | |
| Carnitine[#,*] | 207.6±64.5 | 164.8±24.7 | 305.9±34.5 | 249.3±30.2 | 213.5±46.1 | 380.5±62.8 | 321.5±69.7 | a,b,e | a,b,e,f |
| Choline[#,*] | 130.3±22 | 135.3±17.3 | 220.4±42.7 | 171±26.6 | 130.1±17.8 | 236.5±55.7 | 355.3±55.6 | a,b,e,f | a,b,e,f |
| Citric acid[#] | 301.6±111.1 | 306.7±103.2 | 226.4±77.9 | 266.9±32 | 306.8±86.5 | 360.7±85.2 | 338±91 | e | |
| Creatine[#,*] | 472.5±81.4 | 424.7±67.7 | 559.1±50.7 | 545.1±46 | 456.2±73 | 609.2±38.3 | 573.8±103.4 | a,b,e | a,b,e,f |
| Cytidine 5′-diphosphocholine[#,*] | 39.3±10.5 | 60.1±12.6 | 39.4±16 | 40.4±9.6 | 74.4±18.9 | 58.4±29 | 83.1±18.3 | a,c | a,c,d,f |
| Glycerophosphocholine* | 519.6±112.7 | 649±152.8 | 526.2±98 | 470.6±107.5 | 546.4±103.8 | 660.4±84.8 | 777.5±179.6 | | b,e,f |
| PC(14:0/0:0)* | 47.6±16.1 | 46.2±10.4 | 38.1±12 | 49.9±18.6 | 43.7±7.8 | 70.8±21.1 | 72.5±19.8 | | a,b,e,f |
| PC(16:0/0:0)* | 315.6±106 | 329.4±80 | 304.2±86.1 | 340.4±98.1 | 378.3±82.4 | 441.4±124.2 | 523.6±121 | | b,e,f |
| PC(18:1/0:0)* | 811.6±317.5 | 653±180.9 | 613.7±245.1 | 962.9±363.6 | 772.2±213.8 | 1515.9±586.9 | 1623.9±477.8 | | a,b,e,f |
| PE(20:4/0:0)* | 1799.4±528.7 | 1848.7±472.9 | 1515.3±353 | 2401.9±781 | 2234±514.8 | 2797.3±865.5 | 3385.1±521.4 | | b,e,f |
| PE(22:6/0:0)* | 1218.1±336.8 | 1136.3±223 | 1171.4±177.1 | 1626.9±389.8 | 1416.4±289 | 1683.1±453.1 | 2010.4±483.7 | | b,e,f |
| PE(p-16:0/0:0)[#,*] | 991.2±282.8 | 1086.6±338.7 | 1488.8±340.2 | 1290.6±319.2 | 1539.5±575.5 | 1509.8±200.5 | 2188.3±472.8 | e | b,c,d,e,f |
| Tryptophan[#,*] | 3112.1±569.7 | 3028.5±552.5 | 3525±760.6 | 3858.7±333.1 | 3336.1±678.9 | 3432.7±787.9 | 4536.1±796 | f | b,f |
| NAD[#] | 1526.7±495.1 | 1269.3±353.5 | 1380.2±424.7 | 1588.1±286.4 | 1178.2±371.3 | 1657.5±428.8 | 1603.9±461.6 | e,f | |
| O-Phosphocholine* | 873.9±155.7 | 754.7±128.3 | 771.1±132.6 | 887.2±164.8 | 787.5±121.5 | 980.2±139.2 | 782.3±166.2 | | a,d |
| UDP-GlcA[#,*] | 3777.1±1092.5 | 2253.5±388.1 | 3237±1166.2 | 2731.4±522.3 | 2548.7±421.8 | 3369.3±593.1 | 4305.9±662.6 | a,c, | b,c |

**Table 2.** Cont.

| Name | Cont | 24L | 48L | 72L | 24H | 48H | 72H | Post hoc (1 Gy) | Post hoc (5 Gy) |
|---|---|---|---|---|---|---|---|---|---|
| Arachidonic acid* | 1268±399.8 | 1671.6±445.4 | 1231.4±426.3 | 1683.2±431.6 | 1825.2±510.2 | 1426.1±296.6 | 3145.2±696.9 | | b,c,d,f |
| Arginine#,* | 645.7±131.9 | 732.6±139.4 | 560.7±106.4 | 615.1±173.2 | 621.1±54.9 | 606.8±90.7 | 812.5±131.8 | a | b,d,f |
| D-Alloisoleucine* | 3572.8±549.7 | 3356.7±880.4 | 3534.2±1146.4 | 3951.4±642.1 | 3399.5±534.3 | 3589.1±913.4 | 5502±822.3 | | b,d,f |
| Phenylalanine* | 2804.8±368.5 | 2766.1±399.1 | 2927.8±654.7 | 3111±301.9 | 2834.4±418.1 | 2877.7±413.8 | 3837.9±571.9 | | b,d,f |
| Tyrosine* | 220.6±44.4 | 215.7±45.5 | 229±40.7 | 234.4±40 | 212.8±28 | 212.5±27.7 | 308.9±58.3 | | b,d,f |
| UDP-GalNAc#,* | 48299.1±7411.2 | 40251.3±4034.9 | 49700.8±5848.7 | 43461.7±5832.9 | 33892.6±2454.2 | 48704.9±5218.9 | 80952.5±9008 | a,c | a,b,c,d,-f |

Units: peak area.

Data are given as means ± standard deviations.

Cont, control; 24L, samples irradiated with 1 Gy at 24 h post radiation; 48L, samples irradiated with 1 Gy at 48 h post radiation; 72L, samples irradiated with 1 Gy at 72 h post radiation; 24H, samples irradiated with 5 Gy at 24 h post radiation; 48H, samples irradiated with 5 Gy at 48 h post radiation; 72H, samples irradiated with 5 Gy at 72 h post radiation.

#, and * indicate significant differences between groups irradiated with 1 Gy, and 5 Gy, respectively. Letters in the *post hoc* column indicate significant differences between each group (a, 48 h vs 24 h; b, 72 h vs 48 h; c, Cont vs 24 h; d, 72 h vs 48 h; e, Cont vs 48 h; f, Cont vs 72 h) ($P>0.05$). The $P$-values were calculated by using the Kruskal-Wallis test and Tukey test using rank as *post hoc* test.

doi:10.1371/journal.pone.0113573.t002

reducing power in the cell recovered after exposure to lower-level radiation (1 Gy), but not higher-level radiation (5 Gy). Vitamin B5 is an essential metabolite for the synthesis of coenzyme-A, as well as the synthesis and metabolism of proteins, carbohydrates, and fats [33]. Aqueous vitamin B5 was degraded by free radical ions [34]. In addition, rapidly decreasing ATP and NAD in mouse leukemia cells after exposure to radiation has been reported [35]. Khan et al. [2] reported that energy metabolism in mice was disturbed after exposure to gamma-radiation. Down-regulation of energy metabolites, such as citrate and 2-oxoglutarate, in urine samples was reported in rats after irradiation [16]. Our results on changes in vitamin B5 and related metabolites levels indicate that energy metabolism was disturbed by exposure to radiation. The fibroblasts recovered from the disturbance due to lower-level (but not higher-level) radiation.

Free radical ions damaged cellular molecules and structures, including lipids, proteins, and membranes [36]. Levels of lipids (PC(18:1/0:0), PC(14:0/0:0), PC(16:0/0:0), PE(20:4/0:0), PE(22:6/0:0)), amino acids (arginine, tyrosine, phenylalanine, tryptophan), choline compounds (choline, glycerophosphocholine, cytidine 5′-diphosphocholine), and metabolites structurally related to lipids and amino acids were significantly increased in cells irradiated with 5-Gy γ-radiation and collected at 48 and 72 h or only at 72 h post irradiation (Figure 5). Membrane damage by oxidation releases phospholipids and choline compounds. Increasing levels of phospholipids and choline compounds after exposure to radiation indicated that the cell membrane was damaged by free radical ions induced by radiation. Similarly, previous studies have reported increased triacylglycerol levels in plasma due to the inhibition of lipoprotein lipase in small
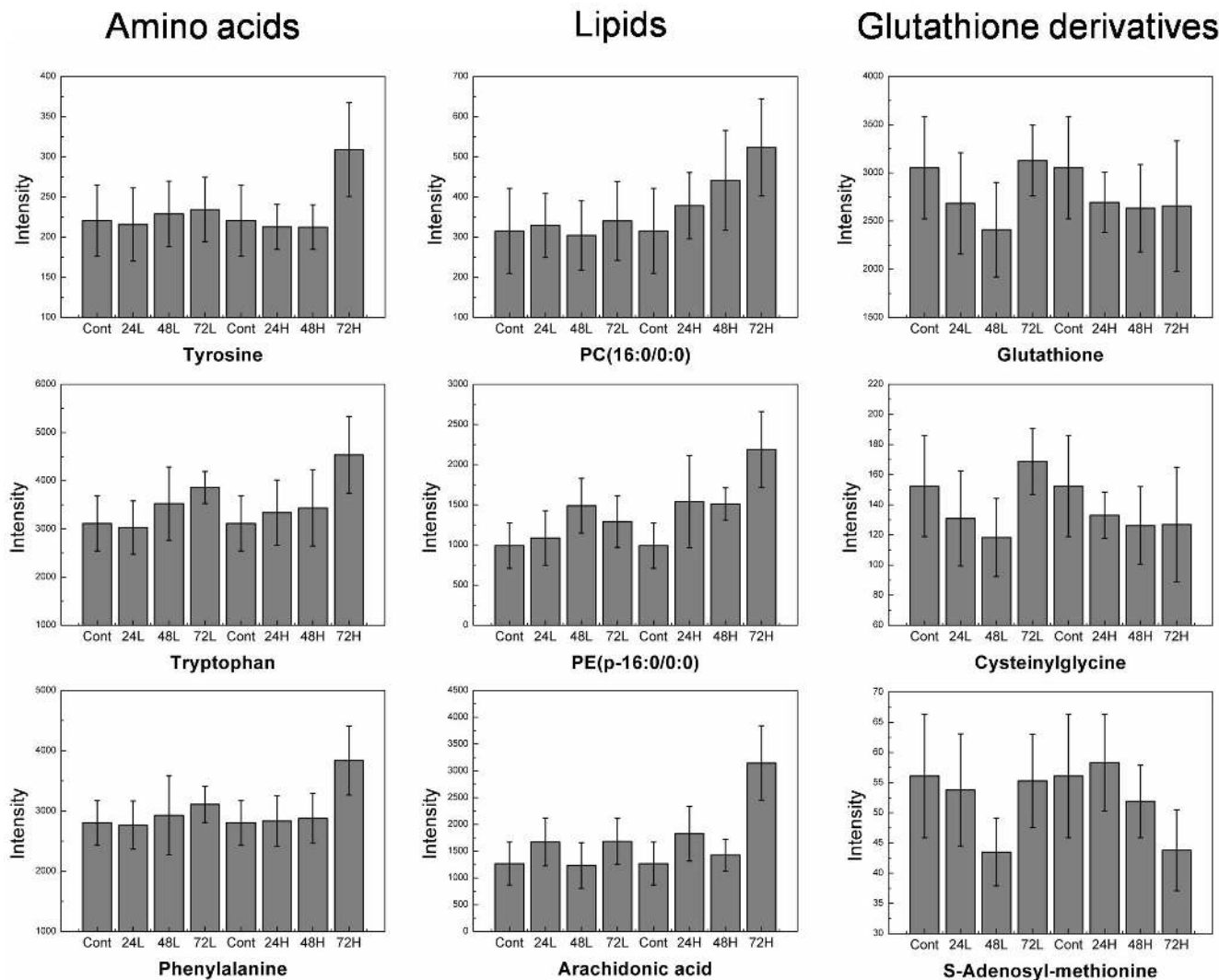
**Figure 5. Quantification of representative metabolites of three classes (amino acids, lipids, and metabolites related to glutathione).**

animals irradiated with γ-rays [37,38]. Many earlier studies have reported the initiation of lipid peroxidation following radiation exposure [39,40]. Khan *et al.* [2] reported that lipid and choline levels increased in the serum of γ-irradiated mice. Holecek et al. [41] described increased amino acid metabolism in rats at 48 h post irradiation with 8 Gy. Radiation induces the degeneration of skeletal muscle, resulting in the release of amino acids from irradiated muscle into the bloodstream [42].

Our results and previous studies indicate that oxygen free radical levels are increased in cells exposed to radiation (Figure 1). These free radicals damage genetic material such as DNA and RNA, and structures such as cell membranes and proteins. The lipids in membranes are degraded, increasing cytoplasmic levels of choline metabolites and lipids. Increasing intracellular amino acids levels are

caused by protein degradation due to radiation and the stress response of the cell. The changes in metabolites, including glutathione, lipids, and amino acids, in cells exposed to γ-radiation indicated that increased peroxidation was increased and damage to membranes and proteins. Following exposure to lower-level radiation (1 Gy) the reduction capacity of free oxidation recovered by 72 h, and membranes and proteins exhibited little damage. However, following exposure to higher-level radiation (5 Gy) the reduction capacity of oxidation did not recover at 72 h, and damage to membranes and proteins was increased markedly. Radiation can induce molecular damages. In addition, radiation may produce ROS, although this does not guarantee cell death. The effect of ROS in cells may differ according to the amount and time of exposure. A well-known example of ROS effects is DNA double strand cleavage. However, DNA cleavage can stimulate normal cellular signaling pathways to induce the so-called "DNA damage response". In this regard damage-induced cellular signaling may contribute to radiation-induced metabolic changes. This possibility is supported by the fact that p53 can respond to radiation-induced DNA damage and regulate various aspects of cellular metabolism [25,43].

## Conclusions

In this study, we investigated the global metabolic responses of human cells to 1- and 5-Gy γ-radiation exposure using a UPLC-QTOF-MS-based metabolomics approach. Changes in global metabolites by radiation showed that cells irradiated with 1 Gy recovered to their normal state, but Cells treated 5 Gy did not. Metabolites associated with antioxidant and ATP synthesis recovered to control levels in cells irradiated with 1 Gy, while amino acids and lipids significantly increased in cells irradiated with 5 Gy. Upon exposure to 1-Gy γ-radiation, glutathione protected the cells from damage by reducing oxygen free radical induced-oxidation, and the levels of glutathione and glutathione derivatives recovered by 72 h after radiation exposure. However, upon exposure to 5 Gy γ-radiation, the capacity for reduction of oxygen free radicals did not recover at 72 h. ATP synthesis recovered in cells irradiated with 1 Gy, but not in cells irradiated with 5 Gy. Changes in lipids and amino acids indicated that higher radiation levels more strongly damaged proteins and cell membranes. This study provides valuable insight into the damage caused by, and recovery from, radiation exposure in terms of metabolic processes. Further studies are required to examine the response to radiation in various organisms or animal models.

## Supporting Information

**Figure S1. PCA score plots were derived from peaks of control groups: A, positive mode; B, negative mode; C, integration of positive and negative modes.** 24C, controls after 24 h; 48C, controls after 48 h; 72C, controls after 72 h. doi:10.1371/journal.pone.0113573.s001 (TIF)

**Figure S2. Total results of *k*-means clustering analysis.** Numbers in front of the heat map are number of cluster from *k*-means clustering analysis. Cont, control; 24L, samples irradiated with 1 Gy at 24 h post radiation; 48L, samples irradiated with 1 Gy at 48 h post radiation; 72L, samples irradiated with 1 Gy at 72 h post radiation; 24H, samples irradiated with 5 Gy at 24 h post radiation; 48H, samples irradiated with 5 Gy at 48 h post radiation; 72H, samples irradiated with 5 Gy at 72 h post radiation.

doi:10.1371/journal.pone.0113573.s002 (TIF)

**Table S1. Summary of number of cells and number of dishes in each group.**
doi:10.1371/journal.pone.0113573.s003 (DOCX)

**Table S2. Peaks associated with identified metabolites.**
doi:10.1371/journal.pone.0113573.s004 (DOCX)

**Table S3. Relative quantification of peaks associated with identified metabolites.**
doi:10.1371/journal.pone.0113573.s005 (DOCX)

## Author Contributions

Conceived and designed the experiments: CMK GSH. Performed the experiments: YKK IJH HWB WGJ HJY SRK EKL. Analyzed the data: YKK GSH. Contributed reagents/materials/analysis tools: CMK GSH. Wrote the paper: YKK IJH CMK GSH.

## References

1. **Coleman CN, Blakely WF, Fike JR, MacVittie TJ, Metting NF, et al.** (2003) Molecular and Cellular Biology of Moderate-Dose (1–10 Gy) Radiation and Potential Mechanisms of Radiation Protection: Report of a Workshop at Bethesda, Maryland, December 17–18, 2001 1. Radiat Res 159: 812–834.

2. **Khan AR, Rana P, Devi MM, Chaturvedi S, Javed S, et al.** (2011) Nuclear magnetic resonance spectroscopy-based metabonomic investigation of biochemical effects in serum of $\gamma$-irradiated mice. Int J Radiat Biol 87: 91–97.

3. **Amundson SA, Fornace AJ Jr** (2003) Monitoring human radiation exposure by gene expression profiling: possibilities and pitfalls. Health Phys 85: 36–42.

4. **Kis E, Szatmári T, Keszei M, Farkas R, Ésik O, et al.** (2006) Microarray analysis of radiation response genes in primary human fibroblasts. Int J Radiat Oncol Biol Phys 66: 1506–1514.

5. **Ménard C, Johann D, Lowenthal M, Muanza T, Sproull M, et al.** (2006) Discovering clinical biomarkers of ionizing radiation exposure with serum proteomic analysis. Cancer Res 66: 1844–1850.

6. **Sreekumar A, Nyati MK, Varambally S, Barrette TR, Ghosh D, et al.** (2001) Profiling of Cancer Cells Using Protein Microarrays Discovery of Novel Radiation-regulated Proteins. Cancer Res 61: 7585–7593.

7. **Patterson AD, Li H, Eichler GS, Krausz KW, Weinstein JN, et al.** (2008) UPLC-ESI-TOFMS-based metabolomics and gene expression dynamics inspector self-organizing metabolomic maps as tools for understanding the cellular response to ionizing radiation. Anal Chem 80: 665–674.

8. **Amundson SA, Do KT, Shahab S, Bittner M, Meltzer P, et al.** (2000) Identification of potential mRNA biomarkers in peripheral blood lymphocytes for human exposure to ionizing radiation. Radiat Res 154: 342–346.

9. **Orešic M, Vidal-Puig A, Hänninen V** (2006) Metabolomic approaches to phenotype characterization and applications to complex diseases. Expert Rev Mol Diagn 6: 575–585.

10. **Raamsdonk LM, Teusink B, Broadhurst D, Zhang N, Hayes A, et al.** (2001) A functional genomics strategy that uses metabolome data to reveal the phenotype of silent mutations. Nature Biotechnol 19: 45–50.

11. **Liu H, Wang Z, Zhang X, Qiao Y, Wu S, et al.** (2013) Selection of candidate radiation biomarkers in the serum of rats exposed to gamma-rays by GC/TOFMS-based metabolomics. Radiat Prot Dosim 154: 9–17.

12. **Tang X, Zheng M, Zhang Y, Fan S, Wang C** (2013) Estimation value of plasma amino acid target analysis to the acute radiation injury early triage in the rat model. Metabolomics 9: 853–863.

13. **Zhang Y, Zhou X, Li C, Wu J, Kuo JE, et al.** (2014) Assessment of early triage for acute radiation injury in rat model based on urinary amino acid target analysis. Mol BioSyst 10: 1441–1449.

14. **Johnson CH, Patterson AD, Krausz KW, Lanz C, Kang DW, et al.** (2011) Radiation metabolomics. 4. UPLC-ESI-QTOFMS-based metabolomics for urinary biomarker discovery in gamma-irradiated rats. Radiat Res 175: 473–484.

15. **Lanz C, Patterson AD, Slavík J, Krausz KW, Ledermann M, et al.** (2009) Radiation metabolomics. 3. Biomarker discovery in the urine of gamma-irradiated rats using a simplified metabolomics protocol of gas chromatography-mass spectrometry combined with random forests machine learning algorithm. Radiat Res 172: 198–212.

16. **Tyburski JB, Patterson AD, Krausz KW, Slavík J, Fornace AJ Jr, et al.** (2008) Radiation metabolomics. 1. Identification of minimally invasive urine biomarkers for gamma-radiation exposure in mice. Radiat Res 170: 1–14.

17. **Tyburski JB, Patterson AD, Krausz KW, Slavík J, Fornace AJ Jr, et al.** (2009) Radiation metabolomics. 2. Dose-and time-dependent urinary excretion of deaminated purines and pyrimidines after sublethal gamma-radiation exposure in mice. Radiat Res 172: 42–57.

18. **Pluskal T, Castillo S, Villar-Briones A, Orešič M** (2010) MZmine 2: modular framework for processing, visualizing, and analyzing mass spectrometry-based molecular profile data. BMC bioinformatics 11: 395.

19. **Veselkov KA, Vingara LK, Masson P, Robinette SL, Want E, et al.** (2011) Optimized preprocessing of ultra-performance liquid chromatography/mass spectrometry urinary metabolic profiles for improved information recovery. Anal Chem 83: 5864–5872.

20. **Fahy E, Subramaniam S, Murphy RC, Nishijima M, Raetz CR, et al.** (2009) Update of the LIPID MAPS comprehensive classification system for lipids. J Lipid Res 50: S9–S14.

21. **Horai H, Arita M, Kanaya S, Nihei Y, Ikeda T, et al.** (2010) MassBank: a public repository for sharing mass spectral data for life sciences. J Mass Spectrom 45: 703–714.

22. **Smith CA, O'Maille G, Want EJ, Qin C, Trauger SA, et al.** (2005) METLIN: a metabolite mass spectral database. Ther Drug Monit 27: 747–751.

23. **Wishart DS, Tzur D, Knox C, Eisner R, Guo AC, et al.** (2007) HMDB: the human metabolome database. Nucl Acids Res 35: D521–D526.

24. **Watrous J, Roach P, Alexandrov T, Heath BS, Yang JY, et al.** (2012) Mass spectral molecular networking of living microbial colonies. Proc Nati Acad Sci U S A 109: E1743–E1752.

25. **Shi Y-Q, Wuergler FE, Blattmann H, Crompton NE** (2001) Distinct apoptotic phenotypes induced by radiation and ceramide in both p53-wild-type and p53-mutated lymphoblastoid cells. Radiat Environ Biophys 40:301–308.

26. **Johnson CH, Patterson AD, Krausz KW, Kalinich JF, Tyburski JB, et al.** (2012) Radiation metabolomics. 5. Identification of urinary biomarkers of ionizing radiation exposure in nonhuman primates by mass spectrometry-based metabolomics. Radiat Res 178: 328–340.

27. **Azzam EI, Jay-Gerin J-P, Pain D** (2012) Ionizing radiation-induced metabolic oxidative stress and prolonged cell injury. Cancer lett 327: 48–60.

28. **Morgan WF, Sowa MB** (2005) Effects of ionizing radiation in nonirradiated cells. Proc Nati Acad Sci U S A 102: 14127–14128.

29. **Couto N, Malys N, Gaskell SJ, Barber J** (2013) Partition and turnover of glutathione reductase from Saccharomyces cerevisiae: a proteomic approach. J Proteome Res 12: 2885–2894.

30. **Chu L, Lai Y, Xu X, Eddy S, Yang S, et al.** (2008) A 52-kDa leucyl aminopeptidase from Treponema denticola is a cysteinylglycinase that mediates the second step of glutathione metabolism. J Biol Chem 283: 19351–19358.

31. **Jösch C, Klotz L-O, Sies H** (2003) Identification of cytosolic leucyl aminopeptidase (EC 3.4. 11.1) as the major cysteinylglycine-hydrolysing activity in rat liver. Biol Chem 384: 213–218.

32. **Tchantchou F, Graves M, Falcone D, Shea TB** (2008) S-adenosylmethionine mediates glutathione efficacy by increasing glutathione S-transferase activity: implications for S-adenosyl methionine as a neuroprotective dietary supplement. J Alzheimer Dis 14: 323–328.

33. **Saliba KJ, Horner HA, Kirk K** (1998) Transport and Metabolism of the Essential Vitamin Pantothenic Acid in Human Erythrocytes Infected with the Malaria ParasitePlasmodium falciparum. J Biol Chem 273: 10190–10195.

34. **Schittl H, Quint R, Getoff N** (2007) Products of aqueous vitamin B5 (pantothenic acid) formed by free radical reactions. Radiat Phys Chem 76: 1594–1599.

35. **Goodwin P, Lewis P, Davies M, Skidmore C, Shall S** (1978) The effect of gamma radiation and neocarzinostatin of NAD and ATP levels in mouse leukaemia cells. Biochim Biophys Acta 543: 576–582.

36. **Cadet J, Bellon S, Douki T, Frelon S, Gasparutto D, et al.** (2004) Radiation-induced DNA damage: formation, measurement, and biochemical features. J Environ Pathol Toxicol Oncol 23:33–43.

37. **Dousset N, Feliste R, Carton M, Douste-Blazy L** (1984) Irradiation-induced free cholesterol accumulation in very-low-density lipoproteins. Role of lipoprotein lipase deficiency. Biochim Biophys Acta 794: 444–453.

38. **Sedlakova A, Borikova K, Ahlers I** (1986) Changes in lipoprotein lipase activity in the adipose tissue and heart of non-lethally X-irradiated rats. Physiol Bohemoslov 35: 400–405.

39. **Leyko W, Bartosz G** (1986) Membrane effects of ionizing radiation and hyperthermia. Int J Radiat Biol Relat Stud Phys Chem Med. 49: 743–770.

40. **Pathak CM, Avti PK, Kumar S, Khanduja KL, Sharma SC** (2007) Whole body exposure to low-dose gamma radiation promotes kidney antioxidant status in Balb/c mice. J Radiat Res 48: 113–120.

41. **Holeček M, Skopec F, Šprongl L, Mraz J, Skalska H, et al.** (2002) Effect of alanyl-glutamine on leucine and protein metabolism in irradiated rats. Amino acids 22: 95–108.

42. **Schwenen M, Altman K, Schröder W** (1989) Radiation-induced increase in the release of amino acids by isolated, perfused skeletal muscle. Int J Radiat Biol 55: 257–269.

43. **Nair B, Krishnan S, Sareddy G, Mann M, Xu B, et al.** (2014) Proline, glutamic acid and leucine-rich protein-1 is essential for optimal p53-mediated DNA damage response. Cell Death Differ 21(9):1409–1418.